Available online at www.sciencedirect.com
SCIENCE DIRECT®
ELSEVIER
Nuclear Instruments and Methods in Physics Research A 518 (2004) 728–737
NUCLEAR INSTRUMENTS & METHODS IN PHYSICS RESEARCH Section A
www.elsevier.com/locate/nima

Ultra-light and stable composite structure to support and cool the ATLAS pixel detector barrel electronics modules

M. Olcese[a,*], C. Caso[a,e], G. Castiglioni[b], R. Cereseto[a], S. Cuneo[a], M. Dameri[a], C. Gemme[a,e], K.-W. Glitza[c], G. Lenzen[c], F. Mora[a], P. Netchaeva[a], W. Ockenfels[d], E. Piano[e], C. Pizzorno[a], R. Puppo[a], A. Rebora[f], L. Rossi[a], J. Thadome[c], F. Vernocchi[a], E. Vigeolas[g], A. Vinci[a]

[a] *INFN, Istituto Nazionale di Fisica Nucleare, I-16146 Genova, Italy*
[b] *PLYFORM, I-20020 Bienate di Magnago (MI), Italy*
[c] *Fachbereich Physik, Bergische Universität, D-42097 Wuppertal, Germany*
[d] *Physikalisches Institut, Universität Bonn, D-53115 Bonn, Germany*
[e] *Department of Physics, Università degli Studi di Genova, I-16146 Genova, Italy*
[f] *Mechanics and Machine Design Department, Università degli Studi di Genova, I-16145 Genova, Italy*
[g] *CPPM, Centre de Physique des Particules de Marseille, F-13288 Marseille, France*

Accepted 29 September 2003

Abstract

The design of an ultra light structure, the so-called "stave", to support and cool the sensitive elements of the Barrel Pixel detector, the innermost part of the ATLAS detector to be installed on the new Large Hadron Collider at CERN (Geneva), is presented.

Very high-dimensional stability, minimization of the material and ability of operating 10 years in a high radiation environment are the key design requirements.

The proposed solution consists of a combination of different carbon-based materials (impregnated carbon–carbon, ultra high modulus carbon fibre composites) coupled to a thin aluminum tube to form a very light support with an integrated cooling channel.

Our design has proven to successfully fulfil the requirements. The extensive prototyping and testing program to fully qualify the design and release the production are discussed.

PACS: 81.70.Bt; 81.70.Pg; 44.50.+f; 65.70.+y

Keywords: LHC; ATLAS; Pixel detector; Mechanics; Cooling; Carbon–carbon; Composites; Impregnation; Al tube

1. Introduction

The Pixel detector [1] is the innermost part of the ATLAS detector to be installed in the new

*Corresponding author. CERN, CH-1211 Geneve 23, Switzerland. Tel./fax: +41227671201.
E-mail address: marco.olcese@cern.ch (M. Olcese).

0168-9002/$ - see front matter © 2003 Published by Elsevier B.V.
doi:10.1016/j.nima.2003.09.071

Large Hadron Collider under construction at the CERN Particle Physics Laboratory in Geneva. Two proton beams will collide in the central point of ATLAS (interaction point).

The ATLAS Pixel Detector (Fig. 1) has to provide critical tracking information for pattern recognition of charged particles generated at the interaction point, with very high efficiency and resolution. The support structure of the pixel electronic sensors has to fulfil tight precision and stability requirements and also has to integrate an efficient cooling system. In fact in the pixel volume a high electronics density produces a relevant amount of heat, which has to be efficiently dissipated in order to keep the pixel sensors at a temperature below 0°C to minimize the radiation damage.

2. The ATLAS Pixel Detector

The ATLAS Pixel Detector consists of over 100 million readout channels organized in an array of 1744 sensitive elements (modules). The module layout has been studied to achieve the required coverage of the solid angle around the interaction point.

The basic structure of the detector consists of a barrel section with three coaxial layers of staves and two disk sections each containing three disks (Fig. 1(a)).

Each barrel layer consists of a cylindrical turbine-like sequence (Fig. 1(b)) of individual support structures (staves) supported on a shell cylinder.

A stave is about 800 mm long and is designed to support and cool 13 detector modules.

3. Requirements and constraints

The pixel detector support structure is subject to tight physics requirements:

- achieve a full coverage of the sensitive area around the interaction point;
- excellent transparency to particles (a "material budget" equivalent in terms of thickness to less

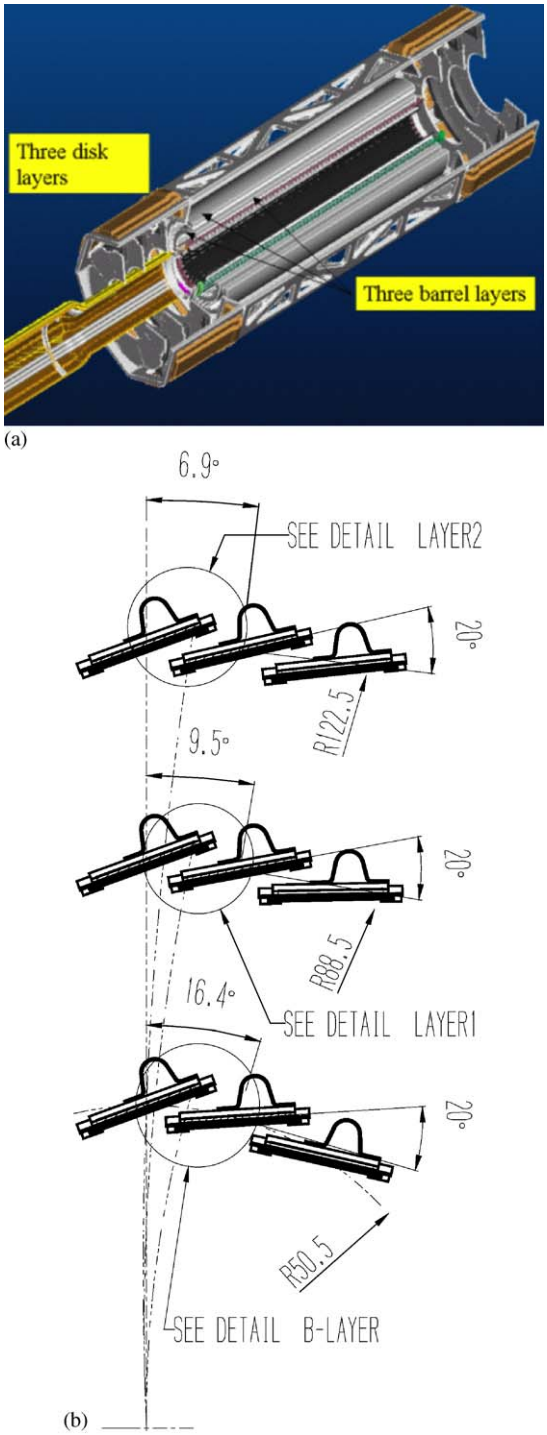

Fig. 1. (a) Cutout view of the ATLAS Pixel Detector overall assembly; (b) partial transverse cross section of the three layers of the barrel Pixel Detector.

than 1% of the radiation length of the material is a common requirement);
- extremely high stability within few microns.

There are also additional constraints due to the installation and operating conditions:

- very limited access to the detector for maintenance: no more than once a year;
- 10 years of expected lifetime;
- high radiation doses: cumulated total dose over 10 years up to 50 mrad;
- high power density dissipated by the electronics (14 kW) in a small volume (0.3 m^3);
- detector modules to be maintained always at a temperature below 0°C.

To fulfil these requirements the mechanical support structure of the detector modules has to be designed according to the following basic rules:

- lightweightness: low mass, materials with high radiation length (X_0);
- high stiffness: small natural deflections, less supports, higher natural frequencies;
- high stability: materials with small coefficients of thermal (CTE) and moisture (CME) expansion;
- radiation hardness;
- reliability: almost maintenance free over 10 years.

4. Pixel sensitive elements

The pixel module is the core unit of the pixel detector (Fig. 2). It is a highly integrated electromechanical unit including:

- a silicon pixel sensor;
- 16 readout chips bump-bonded on the pixel sensor;
- a hybrid circuit wire-bonded to the readout chips, housing the Module Control Chip (MCC) and providing the interfaces to the optical, signal and power cables. Each module dissipates about 8 W over a surface of about 2×6 cm^2.

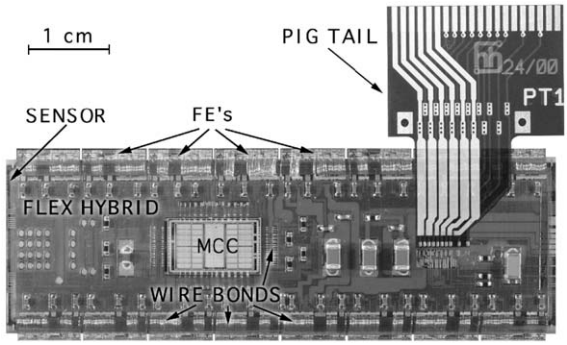

Fig. 2. Typical pixel detector module assembly.

5. The "stave": concept and requirements

The pixel stave is the basic module local support unit of the barrel section of the pixel detector. The stave provides independent support and cooling to 13 modules allowing for a highly modular barrel assembly, which is critical for easy maintenance.

The 13 modules are arranged one after the other along the stave axis and they are partially overlapping in order to achieve the required coverage in the axial direction. Thus the surface of the stave in contact with the modules is stepped and the modules are arranged in a singled layout. A coolant flowing through an integrated cooling tube removes the 100 W of heat dissipated by the electronics.

The barrel layout, the need of minimizing the lateral tilt angle and the requirement for minimum material constraint the cross sectional geometry of the stave and the possible position and size of the cooling channel. These constraints lead to the minimization of the thickness of the stave along radial direction and to offset the position of the cooling channel. Other stave-specific design requirements are summarized in Table 1.

In order to achieve the required temperature uniformity along the stave while introducing as little material as possible, an evaporative cooling system has been adopted [2].

It is based on controlled boiling along the stave cooling channel. A fluoro-carbon fluid (C_3F_8) is delivered to the detector in liquid phase and then it is expanded in a capillary connected to the stave cooling channel, where the boiling conditions are

Table 1
Stave-specific design requirements

Item	Requirements
Max. temp. gradient from coolant to surface	$<15^{\circ}C$
Temperature uniformity on stave surface	$<13^{\circ}C$
Max pressure in cooling channel	16 bar
Max pressure drop in the coolant	170 mbar
Minimum operating temperature	$-35^{\circ}C$
Meet all requirements after	30 temp. cycles from $-25^{\circ}C$ to $+20^{\circ}C$
Local step geometrical tolerance	<50 μm
Overall stave geometrical tolerance	<250 μm
Stability tolerance in Φ	<14 μm
Stability tolerance along the radius	<40 μm
Stability tolerance along axis	<80 μm
Dynamic stability	1st frequency > 100 Hz
Total radiation dose	50 mrad
Max radiation length	$<0.7\%$
Lifetime	> 10 years

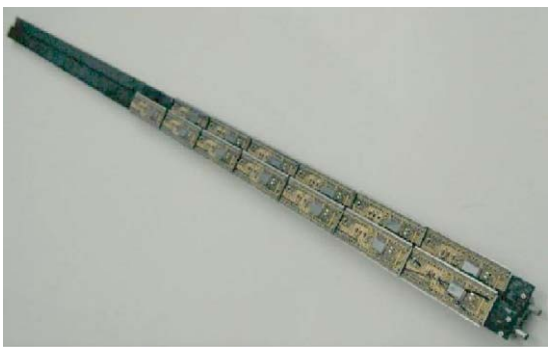

Fig. 3. Bi-stave assembly with dummy modules.

maintained and the temperature is controlled by tuning the vapor pressure in the exhaust tubes.

Before installing on the barrel shell structures, two staves are mounted on a common support to form the so-called "bi-stave" assembly and the cooling tubes are connected in series to the same cooling circuit (see Fig. 3).

6. Design and choice of the materials

The extremely demanding requirements restrict the choice of the materials to just a few options;

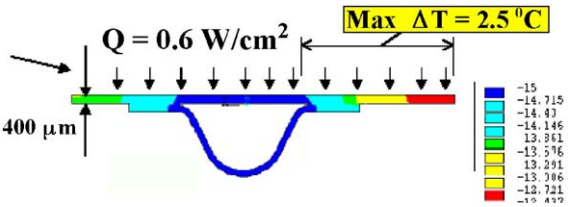

Fig. 4. Typical stave thermal profile showing the right choice of material for the Thermal Management Tile.

this has implied a very long development and optimization process to converge to the best design.

The most difficult design issues to be addressed are cooling and stability. The cooling is critical for the good operation of the modules. The heat is produced over a relatively large area and it has to be transferred with high efficiency to a small cooling tube (Fig. 4).

To minimize the temperature non-uniformities over the modules and the temperature gradient between the module and the coolant, the material of that part of the stave in contact with the module, the so-called Thermal Management Tile (TMT), has to have a good in plane as well as transverse thermal conductivity.

Metallic materials with high radiation length, typically beryllium or aluminum, are in principle good options for the module thermal management. However the metallic materials cannot be used as structural elements for the stave due to their relatively high CTE, not allowing to meet the stability requirement over the 800 mm length.

The only viable options for the stave structure are the carbon-based materials. However standard Carbon Fibre Reinforced Plastics (CFRP) present a low transverse thermal conductivity not suitable for an efficient thermal design of the part in contact with the modules. Carbon–Carbon (C–C) materials have been found to be the best choice for the TMT. The C–C grades with enhanced thermal properties combine good thermal conductivity even in transverse direction to fibres (thermal conductivity 1 or 2 orders of magnitude better than standard CFRP) with excellent mechanical properties, stability and transparency to particles. However C–C materials have two main technological drawbacks limiting their applications:

porosity and difficulty to achieve complex and accurate geometries due to the high temperature manufacturing process. For the stave the porosity issue has been overcome by impregnating the C–C material with a resin to avoid infiltration of the thermal greases and carbon dust release [3]. To allow making the TMT out of standard C–C plates and to provide the required bending stiffness a CFRP omega profile is glued on the backside of the TMT.

An internal thin aluminum tube (Fig. 5) provides the required leak tightness to the cooling channel while introducing small thermal impedance. The aluminum tube is thermally well coupled with the TMT by means of a thin thermal grease layer, which also allows the tube to be weakly coupled structurally with the carbon composite enclosure, thus not affecting the overall stave stability. The final stave design mainly consists of a combination of three different materials each one devoted to a specific function, allowing to make the best use of and to overcome the limitations of the specific properties.

In the following subsections the specific design issues are addressed.

6.1. "Omega" profile

The "omega" profile is made of three layers of unidirectional UHM carbon fibres reinforced pre-preg with cyanate ester resin. The adopted lay-up ($0^\circ - 90^\circ - 0^\circ$), 0.3 mm thick, has been optimized through an extensive design and test program [4].

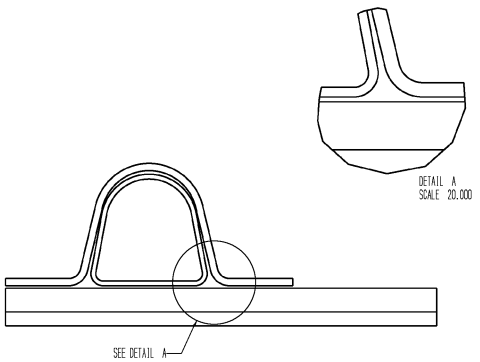

Fig. 5. Stave cross-section showing details of the aluminum tube.

The choice of the pre-preg material and of the lay-up has been made in order to achieve a longitudinal "omega" CTE as close as possible to the CTE of the impregnated C–C, to minimize the distortions due to the cool down. The achieved longitudinal CTE mismatch, less than 1 ppm, allows the structure to fully meet the stability requirements. The fibres are formed to the required shape by means of a graphite mould, whose optimization, as well as the fibres manufacturing process setup, has been carried out during an extensive development program.

The "omega" profile is bonded to the C–C part using Ciba glue Araldite 420 A/B, a radiation-hard 2-component adhesive that features a very high peeling strength. The strength and reliability of the adhesive joint, one of the most critical point of the design, have been deeply investigated and qualified through a very extensive destructive and long term test program, on both test specimens and parts of real-scale prototypes [5].

6.2. Thermal Management Tile (TMT)

The TMT is made of 1502 ZV 22 C–C material from the SGL Company (Germany). The raw material is in form of plates about 6 mm thick. The plates consist of 2-D roving fabric carbon fibre layers overlapped in a phenolic resin matrix, densified and graphitized at high temperature to enhance the thermal properties. The physical properties of the plates are summarized in Table 2.

The plates are first cut in strips and pre-machined, then they are impregnated under vacuum in a special impregnation chamber (Fig. 6).

Table 2
Physical properties of the C–C plates

Property	Units	Specification
Impurity	ppm	<100
Density	g/cm^3	1.76 ± 0.04
Porosity	%	13 ± 2
CTE - in plane	10^{-6} K^{-1}	-0.5 ± 0.2 @ 300°C
CTE - transverse	10^{-6} K^{-1}	12 ± 1 @ 300°C
Kt - in plane	W/m K	250 ± 10 @ 20°C
Kt - transverse	W/m K	30 ± 3 @ 20°C
Youngs modulus-in plane	GPa	120 ± 20

For the impregnation the Ciba epoxy resin system LY 5052 and HY 5052 is used. After the impregnation and curing at 60°C the raw TMTs are machined to the final stepping shape with a CNC milling machine equipped with high speed spindle and diamond coated millers (see Fig. 6).

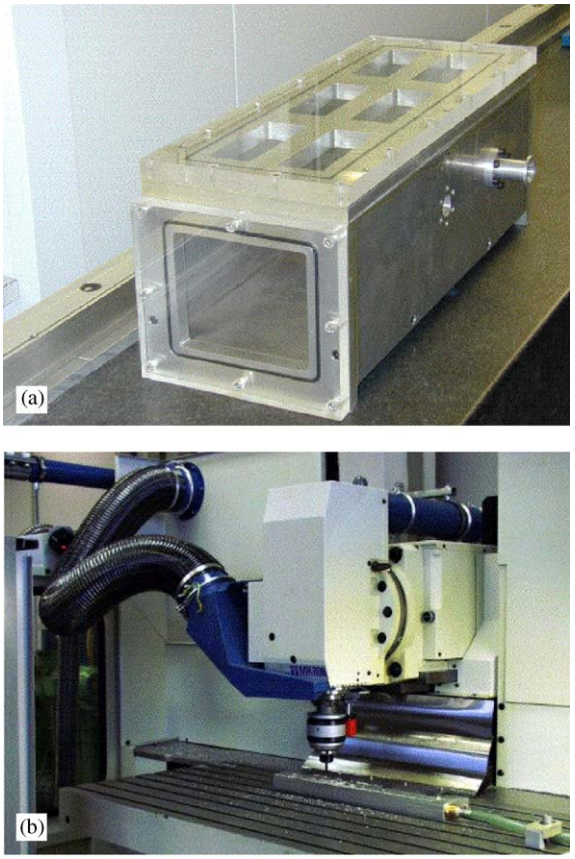

Fig. 6. (a) C–C impregnation chamber and (b) high speed milling machine.

6.3. Cooling tube

The stave cooling circuit is made of a thin aluminum tube (see Fig. 7), shaped to fit inside the inner cross section of the ''omega'' profile. The material chosen is 6060 aluminum alloy. This material shows good extrusion ability at small thickness, low sensitivity to corrosion and high yield stress. The design and the material choice is such that the stave tube operates always in the elastic range up to the maximum fault pressure of 16 bar.

When assembled in the stave the tube perfectly matches on most of the omega surface (Fig. 8).

To account for the different expansions during the cool down and to provide an efficient thermal contact, a 200 μm thick layer of thermal grease (HTCP from Electrolube) is interposed between the flat surface of the tube and the TMT surface. The grease layer is first deposited on the tube, the tube is then laid down on the TMT surface.

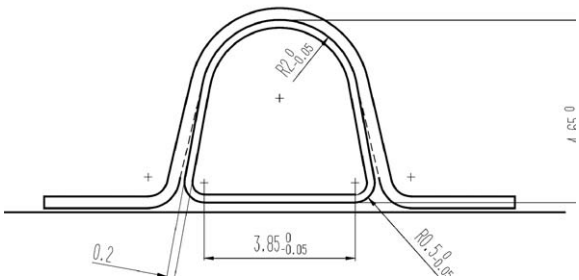

Fig. 8. Stave tube geometry.

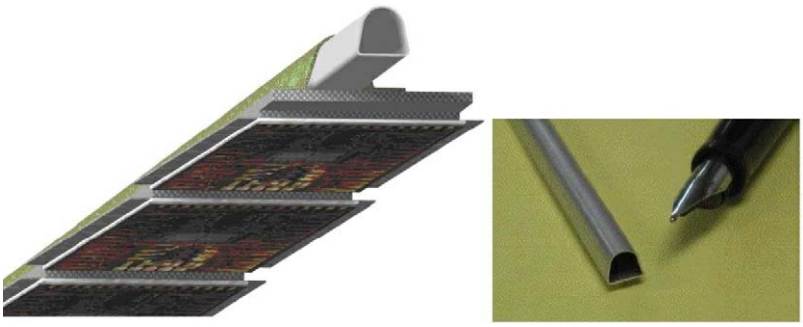

Fig. 7. Details of the stave cooling aluminum tube.

Fig. 9. The end part of an aluminum tube soldered to a nickel plated fitting.

Finally the omega is put on top and bonded down to the TMT surface. Once assembled there is a slight pressure on the grease layer, which allows for good thermal contact and axial compliance. Two aluminum fittings, one per tube end, allow for the connection of the stave tube to the external cooling circuit. The two fittings are nickel plated (11 μm thick layer) (Fig. 9) and then soldered to the aluminum tube, which is also nickel plated over a short length at both ends. The choice of the fitting design and of the joining technique has been done through an extensive test program, which has explored different methods (laser welding, torch brazing) finally converging on the soldering technique allowing for the highest reliability and production yield. After joining the fittings, the tube is finally coated with a thin layer (<15 μm thick) of Parylene, for protection against aluminum-carbon corrosion and for the tube electrical insulation.

7. Analysis

A finite element model of the stave has been made using the ANSYS code,[1] with a very fine mapped mesh to reproduce the small thickness of the different materials. The geometry has been modelled with all its major details.

Some conservative assumptions have been made:

- the aluminum tube has been considered only as an added mass, as shear coupling through the grease layer is difficult to predict;
- the stave was simulated as a beam supported on three points, namely as in the less restrained configuration;
- the electronics modules were simulated as pieces of homogeneous silicon (sensor + electronics chips), with a modified density to take into account the mass of the flex hybrid circuit which does not affect the structural behavior.

The Omega mechanical properties were derived with the classical Schneiders lamination theory [7]. The elastic properties of the C–C were adjusted to account for about the 10% of resin due to impregnation.

For both C–C and omega the CTEs were set to the values measured by a specialized firm.

The model has been used to parametrically analyze the stability of the stave against gravity and cool down loads [6]. The calculated max gravity sag is very small, 0.025 mm, confirming the excellent stiffness of the structure. A small twist around the longitudinal axis due to the marked asymmetry of the cross section is also predicted, but is negligible compared with the sag.

The maximum distortion when the stave is cooled down from 20°C (assembling temperature) to −10°C (operating ambient temperature) is of the same order and in the same direction as the gravity sag. The stave assumes an "S"shape (see Fig. 10), accordingly with the expected bi-laminar effect due to the small but not negligible CTE mismatches between the TMT and the omega and the type of constraint.

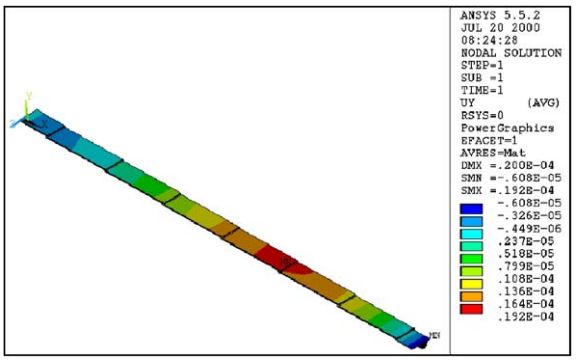

Fig. 10. Cool down simulation: displacements are in [m].

[1] Finite Element Analysis, trademarked by: ANSYS Inc., Southpointe, 275 Technology Drive, Canonsburg, PA 15301.

Being gravity and cool down deflections of the same magnitude, stave bowing disappears when they are in opposite directions, while it doubles when they are in the same direction. Both situations can happen in the actual supporting structure, but anyway the structure is stiff enough to meet the requirements.

Finite element thermal analyses were also carried out to simulate the heat transmission through the C–C tile and the module glue layer as in operating conditions. A single step has only been modelled, since the contribution of the longitudinal heat conduction is negligible. A constant wall temperature on the coolant side has been assumed, which is the case with an evaporative cooling system, and we estimated the highest temperatures on the module surface. Different C–C, with different values of transverse thermal conductivity (ranging from 20 to 35 W/m K), showed hot spots temperature variations within 0.5°C, always complying with the requirements. The central step (Fig. 11) showed the most critical temperature profile.

The results have been confirmed via IR camera imaging, during the cooling tests made on prototypes. A finite elements modal analysis has been performed, assuming two different constraint schemes for the supports: fully restrained and simply supported. The actual constraints will probably react as something in between these two schemes; therefore, the actual first modal frequency should range between the calculated 100 and 150 Hz.

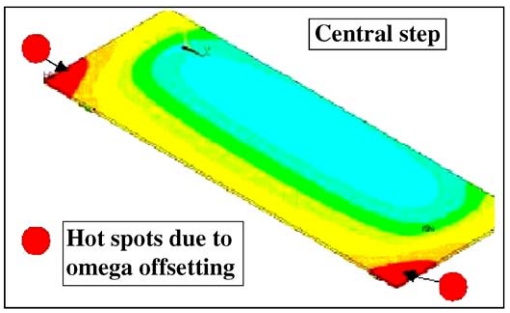

Fig. 11. Calculated temperature distribution on the central step of a stave.

8. Qualification program

Several real scale prototypes of staves have been assembled, and a very comprehensive test program has been carried out to validate the design.

Simulations and measurements were always found in good agreement.

8.1. Cooling tests

Cooling tests have been performed on stave prototypes, equipped with dummy silicon heaters glued with the baseline adhesive; the prototypes have been housed in a cold box to simulate the real operating conditions.

The cooling tests have been carried out with an evaporative cooling system similar to the final one. The system was set to have, at the inlet of the stave, a vapor quality of 0.3 and a temperature of about −22°C. The heaters were powered to reproduce the expected power dissipation of the sensors. Temperature sensors, as well as an infrared camera, allowed measuring the temperature distribution on the stave surface.

Temperature uniformity, maximum temperature gradient between the coolant and the surface and pressure drops along the cooling tube were measured and found to be within the specifications.

Fig. 12 shows a typical temperature distribution along a stave measured at the hottest points on the silicon heaters. Temperature distribution on silicon heaters has also been checked using an infrared camera and found in agreement with our calculations.

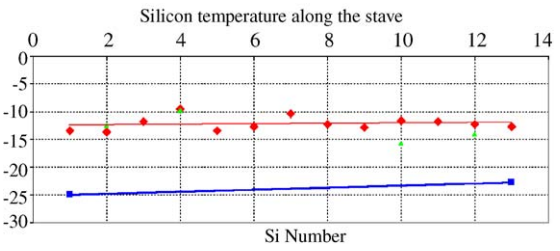

Fig. 12. Measured temperature distribution along the stave at full power with evaporative cooling. The upper points give the temperature on the modules along the stave, with a straight line fit; the lower line gives the coolant temperature.

All the tests have been repeated after irradiation to the maximum expected dose and also after a number of pressure and temperature fatigue cycles likely to be expected over the lifetime of the detector. No change to the thermal performances of the stave was observed, thus proving the good choice of the thermal grease between the tube and the carbon structure.

8.2. Stability tests

Several and very accurate measurements of the stave stability, which is one of the most critical design parameters, have been performed. Both optical interferometer (ESPI) and mechanical (CMM) methods have been applied.

Measurements of displacements on prototypes, constrained as a beam resting on three supports, have been done before and after cooling down from room temperature to -10°C. The typical result of a cool down stability test is shown in Fig. 13, which shows the vertical displacement of the stave central line along the length, compared with the calculations. The calculated distortions fit fairly well with the experimental data, given the small amount of the displacements (max 30 μm) and again the calculation model gave reliable predictions.

The non-symmetric distortion visible in the figure could be explained with the different amount of resin in the impregnated carbon-carbon

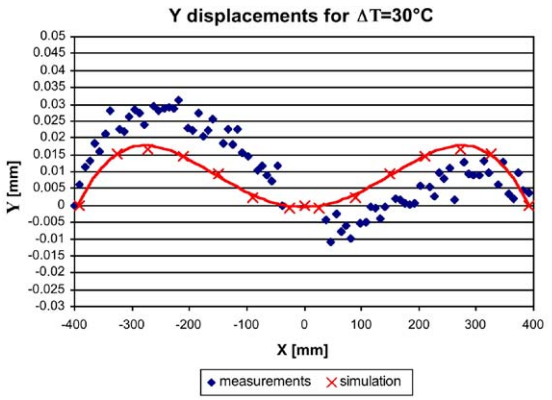

Fig. 13. Predicted (crosses) and measured (diamonds) vertical displacements due to the stave cool down as a function of the position along the stave.

due to the non uniform distribution of the porosity.

8.3. Hydraulic tests

The quality of the joints of the aluminum tube to the end fittings is vital for the reliability of the cooling circuit. The joining method and the final design of the fitting have been selected through a very extensive qualification process.

A specific test protocol has been adopted to simulate the impact of real operating conditions over the entire lifetime; this includes:

- pressure proof test up to 16 bar (maximum fault pressure);
- combined temperature (-30°C… $+20^{\circ}$C) and pressure cycles (1 bar…4 bar);
- thermal shock test to -35°C;
- all tests repeated after irradiation up to 50 mrad.

After testing several prototypes according to this protocol, the adopted design has proven to fully meet all the requirements.

9. Production and quality control

Given the tight requirements, the complexity of the manufacturing process and the relatively high number of items, technical specifications have been developed. This has also given the opportunity to review, document and optimize the pre-production experience. The manufacturing process has been analyzed, identifying the various phases, and procedures have been written down to describe in detail every single step, from raw material purchase to final assembling; critical phases have been identified and associated to quality control steps, ruled by written procedures.

An assembly breakdown structure of the whole detector has been built on the CERN computer server facilities, where every single component has been linked to the relevant drawings and documents. Traceability of the parts has also been foreseen, to allow historical tracking of every single component if non-conformities are found. For this purpose, production and quality control

data-sheet forms, where the critical parameters can be written, have been prepared to record any useful information. A production database, based on the detector assembly breakdown structure, has been built, to allow identification of the single parts produced. Finally, a procedure has been set up to rule non-conformity handling.

As a result, the complete manufacturing process is now extensively documented and all the details will be recorded. All that should allow easier operators training, manufacturing speed-up and better production yield.

10. Conclusions

A support structure (stave) for the pixel electronic sensors of the barrel ATLAS pixel detector has been developed. Several severe constraints are imposed to this support structure by both the physics to be performed and by the foreseen operating conditions. Our project has been especially designed to cope with all of these constraints.

A stave is also intended to include a cooling system to dissipate the heat due to the electronics. The project has then used a combination of carbon-based materials coupled to an aluminum tube for the cooling. Special attention has been paid in the choice of the materials and interfaces in order to reduce as much as possible the mismatch of the various coefficients of thermal expansion.

Extensive laboratory tests and simulations have been made on real scale prototypes to investigate the stave mechanical stability, its thermal performance under cooling and the quality of the system used to connect the stave to the external cooling apparatus.

Our design has demonstrated to fulfill all the imposed design requirements.

Acknowledgements

The authors want to thank their colleagues of the ATLAS pixel team for the many interesting discussions. Thank are also due to F. Gastaldo for his contribution in the early phase of this project.

References

[1] ATLAS Pixel Detector Technical Design Report, CERN/LHCC/98-13, 31 May 1998.
[2] E. Anderssen, et al., Fluorocarbon evaporative cooling developments for the ATLAS pixel and semiconductor tracking detectors, ATLAS-INDET-99-01618, September 1999.
[3] M. Olcese, et al., Impregnation process for thin gas-tight carbon–carbon composite structures, in: Proceedings of the first PRIME 2001 (International Seminar on PRogress in Innovative Manufacturing Engineering).
[4] S. Cuneo, et al., An ultra-light composite structure to support electronic devices in a synchrotron particle detector, INFN/TC-02/05, April 2002.
[5] S. Cuneo, et al., Adhesive joint design of a full composite, ultra-light structure for high energy physics, INFN/TC-02/04, April 2002.
[6] S. Cuneo, et al., Structural analysis of an ultra-light composite structure subject to thermal stress, in: Proceedings Virtual Prototyping Today: Industrial Impact and Future Trends, EnginSoft and modeFrontier Conference and User's Meeting. 2002, Stezzano, Italy, 3–4 October 2002, p. 615.
[7] Structural Materials Handbook: Polymer Composites, Vol. 1, ESA PSS-03-203 Issue 1, 1994.